

## RESEARCH ARTICLE

# MOF Derived $\text{CoFe}_2\text{O}_4$ @Carbon Nanofibers for Supercapacitor Application

T.P. Kamble<sup>1</sup>, S.R. Shingte<sup>2</sup>, V.D. Chavan<sup>3</sup>, Deok-Kee Kim<sup>3</sup>, A.D. Chougale<sup>4</sup>, T.D. Dongale<sup>1</sup>, P.B. Patil<sup>2\*</sup>

**ABSTRACT:** This study presents the synthesis and electrochemical evaluation of MOF-derived  $\text{CoFe}_2\text{O}_4$  nanoparticles anchored on carbon nanofibers ( $\text{CoFe}_2\text{O}_4$ @CNFs) for supercapacitor applications. By integrating hydrothermal and electrospinning techniques, we successfully fabricated  $\text{CoFe}_2\text{O}_4$ @CNFs with enhanced supercapacitive properties. The electrochemical performance of  $\text{CoFe}_2\text{O}_4$ @CNFs was rigorously assessed, revealing a remarkable specific capacitance of 527 F/g at a current density of 1 A/g. Additionally, the electrode demonstrated a power density of 234.93 W/kg and an energy density of 16.58 Wh/kg. These results highlight the synergistic effect of combining MOF-derived bimetallic transition metal oxides with carbon nanofibers, underscoring their potential in advancing supercapacitor technology. The findings suggest that  $\text{CoFe}_2\text{O}_4$ @CNFs can serve as a promising candidate for high-performance energy storage applications, offering a viable pathway to enhance the efficiency and capacity of supercapacitors.

**Keywords:** MOF, Nanofibers, Cobalt ferrite, Carbon Nanofibers, Supercapacitor

Received: 20 January 2024; Revised: 13 February 2024; Accepted: 03 March 2024; Published Online: 20 March, 2024

## 1. INTRODUCTION

Supercapacitors has a potential to provide a solution for efficient energy storage [1], offering rapid charge and discharge capabilities for various applications, including portable electronics and hybrid vehicles [2]. They fall into two categories: electrochemical double-layer capacitors (EDLCs) and pseudocapacitors. EDLCs rely on physical charge separation through ion adsorption. Pseudocapacitors on the other hand store charges through reversible faradic redox reactions [3], commonly employing transition metal oxides, conductive polymers, and other compounds [4].

Presently, scientists are directing their attention towards the utilization of bimetallic transition metal oxides in electrode applications, where a single molecule hosts two

cations. Some of the examples includes  $\text{NiCo}_2\text{O}_4$  [5],  $\text{MnFe}_2\text{O}_4$  [6],  $\text{CuFe}_2\text{O}_4$  [7], and  $\text{CoFe}_2\text{O}_4$  [8]. Among these cobalt ferrite is widely recognized as an inverse spinel structure wherein  $\text{Co}^{2+}$  ions occupy tetrahedral sites, while  $\text{Fe}^{3+}$  ions are distributed among both tetrahedral and cubic crystal structure sites. This unique arrangement potentially enhances redox activity, thereby improving charge storage efficiency [9]. MOFs and materials derived from them are gaining prominence in fine chemical synthesis because of their adaptable properties and potent catalytic capabilities. Nonetheless, while pristine MOFs show promise, their low conductivity limits their effectiveness in supercapacitors. Thus, researchers are exploring the use of MOF-derived nanomaterials, created by annealing MOFs as sacrificial templates, as innovative electrode materials. This approach retains the porous structure characteristic of MOFs while significantly enhancing electrical conductivity [10]. Carbon nanofibers (CNFs) possess desirable qualities for supercapacitors such as excellent electrical conductivity, high specific surface area, and significant aspect ratio. Combining CNFs with MOFs can be an interesting approach to enhance the supercapacitive properties. Electrospinning stands out due to its capability to facilitate the incorporation of CNFs with other materials [11-13].

<sup>1</sup> School of Nanoscience and Technology, Shivaji University, Kolhapur, Maharashtra, 416004, India

<sup>2</sup> Department of Physics, The New College, Shivaji University, Kolhapur, Maharashtra, 416012, India

<sup>3</sup> Department of Electrical Engineering and Convergence Engineering for Intelligent Drone, Sejong University, Seoul, South Korea.

<sup>4</sup> Department of Chemistry, The New College, Shivaji University, Kolhapur, Maharashtra, 416012, India.

\*Author to whom correspondence should be addressed:  
prashantphy@gmail.com (P. B. Patil)

In this study, we synthesized CoFe<sub>2</sub>O<sub>4</sub> nanoparticles anchored carbon nanofibers (CoFe<sub>2</sub>O<sub>4</sub>@CNFs). For this CoFe MOF was prepared by hydrothermal method. CoFe MOF was then used in electrospinning technique to anchor MOF derived CoFe<sub>2</sub>O<sub>4</sub> nanoparticles on carbon nanofibers. Supercapacitive performance of CoFe<sub>2</sub>O<sub>4</sub>@CNFs has been thoroughly investigated.

## 2. EXPERIMENTAL DETAILS

### 2.1. Chemicals

Cobalt nitrate hexahydrate (Co (NO<sub>3</sub>)<sub>2</sub>·6H<sub>2</sub>O) obtained from SRL Pvt Ltd, along with iron nitrate nonahydrate (Fe (NO<sub>3</sub>)<sub>2</sub>·9H<sub>2</sub>O), p-phthalic acid (PTA) and polyacrylonitrile (PAN, Mw–150000) from Sigma Aldrich, were used. N, N-dimethylformamide (DMF) from SRL, potassium hydroxide (KOH) from Loba Chemie Pvt Ltd, and double distilled water (DDW) were utilized for solution preparations. For electrode assembly, commercial Ni foam, polyvinylidene fluoride (PVDF), activated carbon, and N-methyl-2-pyrrolidone (NMP) were employed.

### 2.2. Synthesis of CoFe MOF

To synthesize the CoFe metal-organic framework (MOF), cobalt nitrate hexahydrate and iron nitrate nonahydrate were dissolved in DMF containing terephthalic acid. This mixture was subjected to hydrothermal treatment at 150 °C for 8 hours. The resulting CoFe MOF powder was thoroughly washed with DMF and DDW to remove any unreacted precursors and impurities.

### 2.3. Synthesis of CoFe<sub>2</sub>O<sub>4</sub>@CNFs

The MOF-derived CoFe<sub>2</sub>O<sub>4</sub>@carbon nanofibers (CoFe<sub>2</sub>O<sub>4</sub>@CNFs) were prepared using electrospinning followed by annealing. Initially, PAN and CoFe MOF were separately dissolved in DMF to form uniform solutions. These solutions were then mixed and electrospun onto aluminum foil to form a nanofiber mat. The electrospun mat was first calcined at 240 °C in air for 2 hours to stabilize the structure and remove any residual solvent. Subsequently, the fibers were annealed in nitrogen at 600 °C, resulting in the formation of CoFe<sub>2</sub>O<sub>4</sub>@CNFs.

### 2.4. Characterizations

The surface morphology of the CoFe<sub>2</sub>O<sub>4</sub>@CNFs was examined using a field emission scanning electron microscope (FESEM, Hitachi SU 8010). The detailed microstructure was further investigated using a transmission electron microscope (TEM, Hitachi/HF-3300, 300 kV). These techniques provided comprehensive insights into the structural and morphological attributes of the synthesized

nanofibers.

## 2.5. Electrochemical measurements

For the fabrication of the electrodes, a homogeneous slurry was prepared by mixing CoFe<sub>2</sub>O<sub>4</sub>@CNFs, activated carbon, and PVDF in a weight ratio of 80:10:10 in N-methyl-2-pyrrolidone. This slurry was then brush-coated onto a nickel foam substrate (1 × 3 cm<sup>2</sup>) and allowed to dry overnight at 50 °C. Electrochemical measurements were conducted using a Metrohm Autolab PGSTAT204 workstation in a 1 M KOH aqueous solution. A three-electrode configuration was employed, where Ag/AgCl and Pt wire served as the reference and counter electrodes, respectively. This setup allowed for a detailed evaluation of the electrochemical performance of the CoFe<sub>2</sub>O<sub>4</sub>@CNF electrodes.

## 3. RESULTS AND DISCUSSION

### 3.1. Surface Morphology and Microstructure Analysis

The surface morphology of the CoFe<sub>2</sub>O<sub>4</sub>@CNFs was thoroughly examined using Field Emission Scanning Electron Microscopy (FE-SEM). The FE-SEM images at low (Figure 1(a)) and high magnifications (Figure 1(b)) provide a detailed visualization of the synthesized nanostructures. At low magnification (Figure 1(a)), the FE-SEM images reveal the presence of carbon nanofibers that extend several micrometers in length. These long fibers create a web-like structure, which is advantageous for forming an interconnected network. Such a network is essential for enhancing the overall conductivity of the material, as it facilitates efficient electron transport pathways. When observed at higher magnification (Figure 1(b)), the FE-SEM images provide a closer look at the surface features of the carbon nanofibers. It becomes evident that the CoFe<sub>2</sub>O<sub>4</sub> nanoparticles are well-dispersed and firmly anchored on the surfaces of the carbon nanofibers. These nanoparticles appear as bright spots due to their different electron scattering properties compared to the carbon matrix. The agglomeration of CoFe<sub>2</sub>O<sub>4</sub> nanoparticles on the nanofibers suggests a strong interaction between the nanoparticles and the carbon matrix, which is beneficial for maintaining structural stability during electrochemical processes. The average diameter of the carbon nanofibers was measured to be approximately 154 nm. This nanoscale diameter is beneficial for supercapacitor applications as it provides a high surface area-to-volume ratio. A larger surface area allows for more efficient interaction with the electrolyte, leading to increased charge storage capacity.

To gain deeper insights into the microstructure of the CoFe<sub>2</sub>O<sub>4</sub>@CNFs, Transmission Electron Microscopy (TEM) was utilized. The TEM micrographs at low (Figure 2(a)) and high magnifications (Figure 2(b)) provide a comprehensive

view of the internal structure of composite. At low magnification (Figure 2(a)), the TEM images reveal the overall distribution and integration of  $\text{CoFe}_2\text{O}_4$  nanoparticles within the carbon nanofibers. The nanoparticles are uniformly embedded in the carbon matrix, confirming successful incorporation during the synthesis process. This uniform distribution is crucial for ensuring consistent electrochemical performance across the entire electrode material. High magnification TEM images (Figure 2(b)) offer a closer examination of the  $\text{CoFe}_2\text{O}_4$  nanoparticles within the carbon nanofibers. The nanoparticles appear as distinct, dark spots embedded in the lighter carbon matrix. The close proximity and intimate contact between the nanoparticles and the carbon fibers are evident, which facilitates efficient electron transfer and ionic diffusion during electrochemical processes. The high-resolution images also indicate that the nanoparticles maintain their structural integrity and crystalline nature even after the high-temperature annealing

process, which is essential for maintaining their electrochemical activity. The Selected Area Electron Diffraction (SAED) pattern, depicted in Figure 2(c), provides further confirmation of the crystalline nature of the  $\text{CoFe}_2\text{O}_4$  nanoparticles. The SAED pattern exhibits distinct rings that correspond to the (311), (220), and (422) crystal planes of the cubic crystal lattice of the  $\text{CoFe}_2\text{O}_4$  phase. These planes are characteristic of the spinel structure of  $\text{CoFe}_2\text{O}_4$ , with a space group of  $Fd-3m$ , as indexed by the Joint Committee on Powder Diffraction Standards (JCPDS No. 00-002-1045). The presence of these diffraction rings in the SAED pattern indicates the highly crystalline nature of the  $\text{CoFe}_2\text{O}_4$  nanoparticles. The well-defined rings suggest that the nanoparticles are well-ordered and possess a high degree of crystallinity, which is beneficial for their electrochemical performance. High crystallinity often correlates with improved electronic conductivity and stability, both of which are critical for supercapacitor applications.

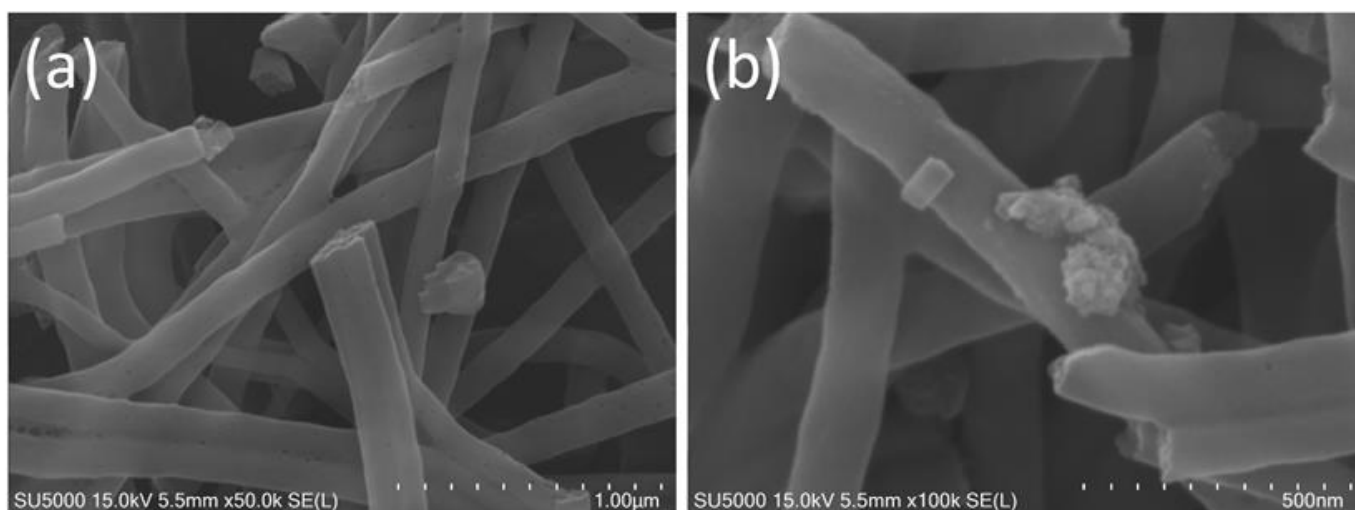


**Fig. 1.** (a) Low and (b) high magnification FE-SEM images of  $\text{CoFe}_2\text{O}_4$ @CNFs.

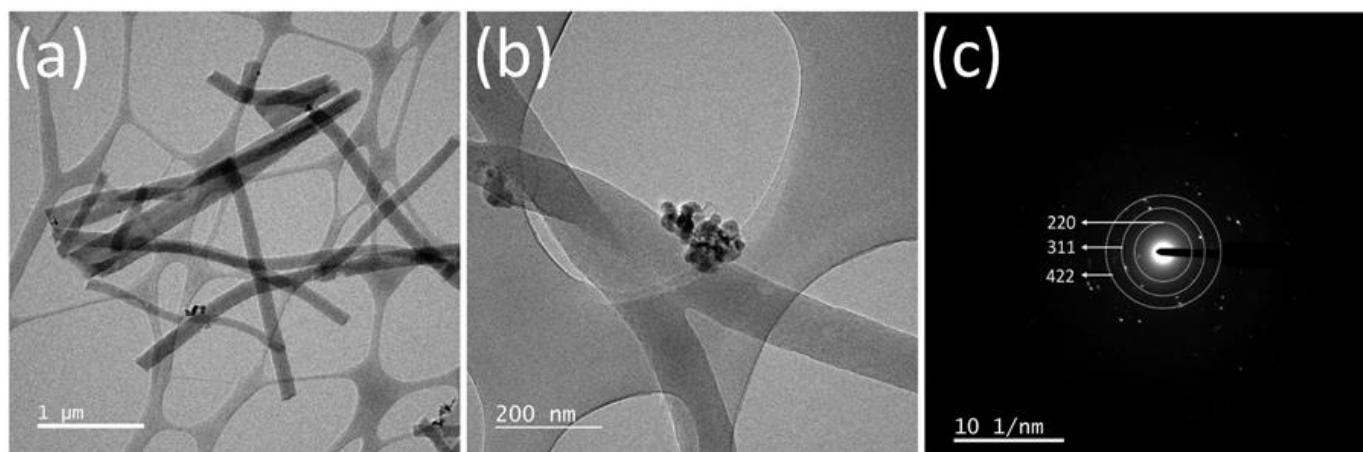


**Fig. 2.** TEM images at (a) low, and (b) high magnifications and (c) SAED pattern of  $\text{CoFe}_2\text{O}_4$ @CNFs.

### 3.2. Electrochemical Performance: Cyclic Voltammetry Analysis

The electrochemical capacitive properties of CoFe<sub>2</sub>O<sub>4</sub>@CNFs were thoroughly evaluated using cyclic voltammetry (CV) in a 1 M KOH aqueous electrolyte solution. This analysis is crucial for understanding the charge storage capabilities and overall performance of the material in supercapacitor applications.

The CV curve at a scan rate of 50 mV/s is presented in Figure 3(A). This curve exhibits distinct redox peaks, which are indicative of pseudocapacitance [14]. Pseudocapacitive behavior arises from faradic redox reactions occurring at the surface of the electrode material. The presence of these peaks suggests that the CoFe<sub>2</sub>O<sub>4</sub> nanoparticles undergo reversible oxidation and reduction processes, contributing significantly to the overall capacitance. This type of capacitance is often associated with higher energy densities compared to electric double-layer capacitance, making the material particularly promising for energy storage applications. The CV curves measured at different scan rates (10-100 mV/s) are shown in Figure 3B. These curves maintain a consistent shape across the various scan rates, which indicates good reversibility and stability of the charge storage mechanism. This consistency is crucial for practical supercapacitor applications, where the electrode material must reliably operate under different charge-discharge rates.

The rate capability of the CoFe<sub>2</sub>O<sub>4</sub>@CNFs electrode is further demonstrated in Figure 3(B). As the scan rate increases, the area under the CV curves also increases. This behavior suggests that the material can effectively store and release charge even at higher scan rates, which is essential for applications requiring quick energy delivery, such as in power tools or electric vehicles. The increase in CV area with higher scan rates is attributed to the combined effects of ion diffusion, surface adsorption, and charge transfer processes. At lower scan rates, ions have sufficient time to diffuse into the deeper parts of the electrode material, leading to higher capacitance. However, at higher scan rates, the process becomes more surface-limited as ions do not have enough time to penetrate deeply. This results in a decrease in specific capacitance, as the charge storage becomes more reliant on surface adsorption and rapid charge transfer processes [15].

### 3.3. Electrochemical Performance: Galvanostatic Charge-Discharge (GCD) Analysis

The electrochemical performance of CoFe<sub>2</sub>O<sub>4</sub>@CNFs was extensively evaluated using galvanostatic charge-discharge (GCD) measurements. The GCD curves, shown in Figure 4(A), exhibit nonlinear characteristics with distinct charge and discharge plateaus, which are indicative of typical faradaic behavior associated with pseudocapacitors. This faradaic behavior is essential for materials used in supercapacitors as it enhances the energy storage capacity through redox reactions [16]. The specific capacitance values of the CoFe<sub>2</sub>O<sub>4</sub>@CNFs were calculated from the GCD

curves at various current densities over a potential range of 0.0 to 0.47 V. The specific capacitance (Cs) is determined using the equation:

$$\text{Specific Capacitance } (C_s) = \frac{I \Delta t}{m \Delta V}$$

where  $I$  is the discharge current,  $\Delta t$  is the discharge duration,  $\Delta V$  is the voltage window, and  $m$  represents the mass of the active material. At a current density of 1 A/g, the specific capacitance of CoFe<sub>2</sub>O<sub>4</sub>@CNFs was calculated to be 527 F/g. This high specific capacitance highlights the excellent charge storage capability of the material. The specific capacitance values at different current densities are presented in Table 1.

The decline in specific capacitance observed at higher current densities can be attributed to several factors. At higher current densities, the faradaic reactions of the active materials may not proceed to completion within the limited time available, leading to lower utilization of the active material. Additionally, increased resistance at high current densities can impede charge transfer processes. Another contributing factor is the preferential engagement of only the outer surface of the electrode for redox reactions, which limits the overall capacitance [17].

Energy density (ED) and power density (PD) are critical parameters for evaluating the performance of supercapacitors. These were calculated using the following equations:

$$\text{Energy Density } (ED) = \frac{0.5 C_s (V_2 - V_1)^2}{3.6}$$

$$\text{Power Density } (PD) = \frac{ED}{\Delta T \cdot 3600}$$

The calculated energy and power densities at different current densities are presented in Table 1. At a current density of 1 A/g, the energy density was found to be 16.58 Wh/kg, and the power density was 234.9 W/kg. These values demonstrate the material's potential for high-energy and high-power applications [18].

To further understand the electrochemical behavior, Electrochemical Impedance Spectroscopy (EIS) was performed. The EIS data, collected using an AC voltage of 5 mV over frequencies ranging from 0.01 Hz to 100 kHz, is represented in the Nyquist plot shown in Figure 4(B). The Nyquist plot reveals two main regions: a semi-circle at high frequencies and a straight line at low frequencies.

The semi-circle at high frequencies is indicative of the charge transfer process, representing the resistance to redox probe transfer at the electrode interface. The diameter of the semi-circle corresponds to the charge transfer resistance (R<sub>ct</sub>), which was measured to be 32.84 Ω/cm<sup>2</sup>. The series resistance (R<sub>s</sub>), encompassing ionic resistance of the electrolyte, electrode material resistance, and contact resistance, was measured to be 1.59 Ω/cm<sup>2</sup>. These resistance values are crucial for understanding the impedance characteristics of the material and its suitability for supercapacitor applications [19, 20].

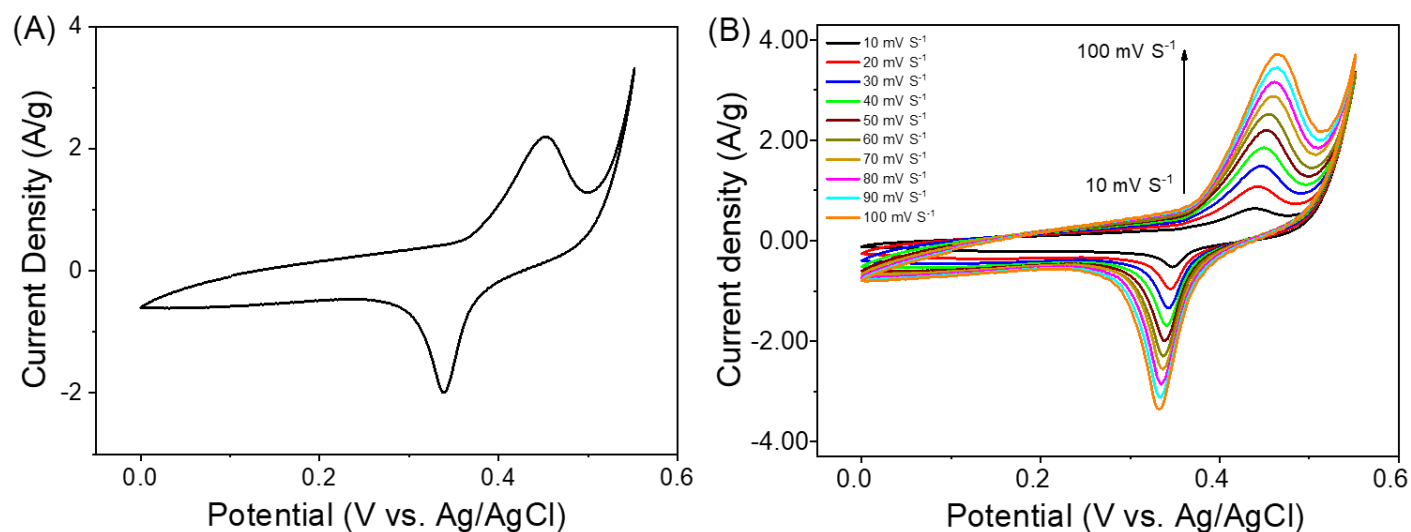


**Fig. 3.** (A) CV curve at 50 mV/s and (B) the CV curves at various scan rates in 1 M KOH of  $\text{CoFe}_2\text{O}_4$ @CNFs.

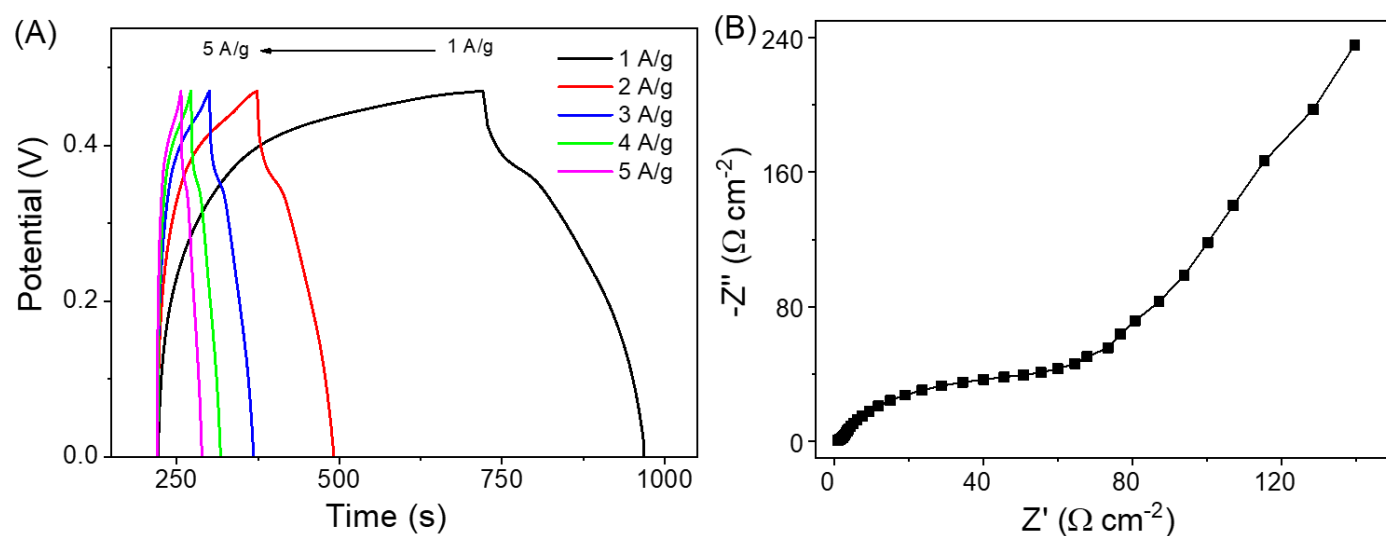


**Fig. 4.** (A) GCD curves at different current densities and (B) the Nyquist plot of  $\text{CoFe}_2\text{O}_4$ @CNFs.

**Table 1.** Specific capacitance, energy density, and power density of  $\text{CoFe}_2\text{O}_4$ @CNFs electrode at different current densities.

| Current density (A/g) | Specific capacitance (F/g) | Energy density (Wh/Kg) | Power density (W/Kg) |
|-----------------------|----------------------------|------------------------|----------------------|
| 1                     | 527                        | 16.58                  | 234.9                |
| 2                     | 493                        | 15.14                  | 269.8                |
| 3                     | 446                        | 13.70                  | 704.5                |
| 4                     | 374                        | 11.5                   | 940                  |
| 5                     | 351                        | 10.76                  | 1173.8               |

The linear segment with a 45° slope observed in the Nyquist plot at low frequencies is indicative of Warburg impedance, suggesting diffusion-controlled processes. This behavior further confirms the pseudocapacitive nature of the CoFe<sub>2</sub>O<sub>4</sub>@CNFs electrode material. The findings from the EIS analysis are consistent with those obtained from the CV and GCD experiments, reinforcing the material's potential for use in supercapacitors.

#### 4. CONCLUSIONS

In conclusion, we have successfully developed a facile and efficient strategy to anchor MOF-derived CoFe<sub>2</sub>O<sub>4</sub> nanoparticles onto carbon nanofibers using the electrospinning technique for supercapacitor applications. This innovative approach combines the advantageous properties of fibrous structured carbon with the unique characteristics of MOF-derived CoFe<sub>2</sub>O<sub>4</sub>, resulting in a composite material with a large surface area and abundant exposed active sites, which are crucial for superior electrochemical performance. The CoFe<sub>2</sub>O<sub>4</sub>@CNFs demonstrated an impressive specific capacitance of 527 F/g at a current density of 1 A/g, showcasing their excellent charge storage capability. Additionally, the material exhibited a high energy density of 16.58 Wh/kg and a power density of 234.93 W/kg, indicating its potential for high-energy and high-power applications. These electrochemical properties make CoFe<sub>2</sub>O<sub>4</sub>@CNFs a promising candidate for next-generation supercapacitors. The combination of carbon nanofibers and MOF-derived CoFe<sub>2</sub>O<sub>4</sub> nanoparticles not only enhances the overall electrochemical performance but also provides a robust and stable structure, ensuring long-term durability and efficiency. This work highlights the potential of metal oxide nanoparticle-modified electrospun carbon nanofibers in supercapacitive applications and paves the way for the preparation and utilization of MOF-derived materials in advanced energy storage systems. The study presents a significant advancement in the field of supercapacitors, demonstrating the feasibility and effectiveness of using MOF-derived CoFe<sub>2</sub>O<sub>4</sub> nanoparticles anchored on carbon nanofibers. This approach offers a new pathway for the development of high-performance, sustainable, and cost-effective energy storage solutions, contributing to the ongoing efforts to meet the growing demand for efficient and reliable energy storage technologies.

#### CONFLICT OF INTEREST

The authors declare that there is no conflict of interests.

#### ACKNOWLEDGEMENTS

This work is supported by the Science and Engineering Research Board, Department SARTHI for the fellowship. V.D. Chavan and Deok-Kee Kim acknowledge the financial

support provided by the National Research Foundation of Korea (NRF), funded by the Ministry of Science and ICT (2016RID1A1B01009537).

#### REFERENCES

- [1] Kakaei, K., Esrafil, M.D. and Ehsani, A., **2019**. Graphene-based electrochemical supercapacitors. In *Interface science and technology* (Vol. 27, pp. 339-386). Elsevier.
- [2] Snook, G.A., Kao, P. and Best, A.S., **2011**. Conducting-polymer-based supercapacitor devices and electrodes. *Journal of power sources*, 196(1), pp.1-12.
- [3] Nikam, S.M., Sharma, A., Rahaman, M., Teli, A.M., Mujawar, S.H., Zahn, D.R.T., Patil, P.S., Sahoo, S.C., Salvan, G. and Patil, P.B., **2020**. Pulsed laser deposited CoFe<sub>2</sub>O<sub>4</sub> thin films as supercapacitor electrodes. *RSC advances*, 10(33), pp.19353-19359.
- [4] Patil, P.D., Shingte, S.R., Karade, V.C., Kim, J.H., Dongale, T.D., Mujawar, S.H., Patil, A.M. and Patil, P.B., **2021**. Effect of annealing temperature on morphologies of metal organic framework derived NiFe<sub>2</sub>O<sub>4</sub> for supercapacitor application. *Journal of Energy Storage*, 40, p.102821.
- [5] Wang, Q., Wang, X., Xu, J., Ouyang, X., Hou, X., Chen, D., Wang, R. and Shen, G., **2014**. Flexible coaxial-type fiber supercapacitor based on NiCo<sub>2</sub>O<sub>4</sub> nanosheets electrodes. *Nano Energy*, 8, pp.44-51.
- [6] Sankar, K.V. and Selvan, R.K., **2015**. The ternary MnFe<sub>2</sub>O<sub>4</sub>/graphene/polyaniline hybrid composite as negative electrode for supercapacitors. *Journal of Power Sources*, 275, pp.399-407.
- [7] Giri, S., Ghosh, D., Kharitonov, A.P. and Das, C.K., **2012**. Study of copper ferrite nanowire formation in presence of carbon nanotubes and influence of fluorination on high performance supercapacitor energy storage application. *Functional Materials Letters*, 5(04), p.1250046.
- [8] Lv, L., Xu, Q., Ding, R., Qi, L. and Wang, H., **2013**. Chemical synthesis of mesoporous CoFe<sub>2</sub>O<sub>4</sub> nanoparticles as promising bifunctional electrode materials for supercapacitors. *Materials letters*, 111, pp.35-38.
- [9] Xiong, P., Chen, Q., He, M., Sun, X. and Wang, X., **2012**. Cobalt ferrite-polyaniline heteroarchitecture: a magnetically recyclable photocatalyst with highly enhanced performances. *Journal of Materials Chemistry*, 22(34), pp.17485-17493.
- [10] Yan, J., Liu, T., Liu, X., Yan, Y. and Huang, Y., **2022**. Metal-organic framework-based materials for flexible supercapacitor application. *Coordination Chemistry Reviews*, 452, p.214300.
- [11] Lu, X., Wang, C., Favier, F. and Pinna, N., **2017**. Electrospun nanomaterials for supercapacitor electrodes: designed architectures and electrochemical performance. *Advanced Energy Materials*, 7(2), p.1601301.

- [12] Nie, G., Lu, X., Chi, M., Gao, M. and Wang, C., **2018**. General synthesis of hierarchical C/MO<sub>x</sub>@ MnO<sub>2</sub> (M= Mn, Cu, Co) composite nanofibers for high-performance supercapacitor electrodes. *Journal of colloid and interface science*, 509, pp.235-244.
- [13] Nie, G., Zhao, X., Luan, Y., Jiang, J., Kou, Z. and Wang, J., **2020**. Key issues facing electrospun carbon nanofibers in energy applications: on-going approaches and challenges. *Nanoscale*, 12(25), pp.13225-13248.
- [14] Lee, D.Y., Shinde, D.V., Kim, E.K., Lee, W., Oh, I.W., Shrestha, N.K., Lee, J.K. and Han, S.H., **2013**. Supercapacitive property of metal-organic-frameworks with different pore dimensions and morphology. *Microporous and mesoporous materials*, 171, pp.53-57.
- [15] Liu, J., Wang, J., Xu, C., Jiang, H., Li, C., Zhang, L., Lin, J. and Shen, Z.X., **2018**. Advanced energy storage devices: basic principles, analytical methods, and rational materials design. *Advanced science*, 5(1), p.1700322.
- [16] Xu, K., Ma, S., Shen, Y., Ren, Q., Yang, J., Chen, X. and Hu, J., **2019**. CuCo<sub>2</sub>O<sub>4</sub> nanowire arrays wrapped in metal oxide nanosheets as hierarchical multicomponent electrodes for supercapacitors. *Chemical Engineering Journal*, 369, pp.363-369.
- [17] Alkhalaf, S., Ranaweera, C.K., Kahol, P.K., Siam, K., Adhikari, H., Mishra, S.R., Perez, F., Gupta, B.K., Ramasamy, K. and Gupta, R.K., **2017**. Electrochemical energy storage performance of electrospun CoMn<sub>2</sub>O<sub>4</sub> nanofibers. *Journal of Alloys and Compounds*, 692, pp.59-66.
- [18] Zain, Z.M. and Zakaria, N., **2014**. Hydrogen peroxide impedimetric detection on poly-ortho-phenylenediamine modified platinum disk microelectrode. *Malaysian Journal of Analytical Sciences*, 18(1), pp.107-115.
- [19] Salleh, N.A., Kheawhom, S. and Mohamad, A.A., **2020**. Characterizations of nickel mesh and nickel foam current collectors for supercapacitor application. *Arabian Journal of Chemistry*, 13(8), pp.6838-6846.
- [20] Mei, B.A., Lau, J., Lin, T., Tolbert, S.H., Dunn, B.S. and Pilon, L., **2018**. Physical interpretations of electrochemical impedance spectroscopy of redox active electrodes for electrical energy storage. *The Journal of Physical Chemistry C*, 122(43), pp.24499-24511.